



Article

Pristine and Coated Carbon Nanotube Sheets—Characterization and Potential Applications

Prakash Giri , Irwin Gill, Morgan Swensgard, Alexandra Kaiser, Audrey Rust, Brian Stuparyk, Andrew Fisher, Justice Williams, Katie Renoit, Eleanor Kreeb, Corentin Lavenan and Mark J. Schulz *

Nanoworld Laboratories, University of Cincinnati, Cincinnati, OH 45221, USA; giriph@mail.uc.edu (P.G.); kaisera9@mail.uc.edu (A.K.); rustal@mail.uc.edu (A.R.)

* Correspondence: mark.j.schulz@uc.edu

Abstract: A carbon nanotube (CNT) sheet is a nonwoven fabric that is being evaluated for use in different textile applications. Several properties of pristine CNT sheets and CNT sheets coated with a polysilazane sealant and coating were measured and compared in the paper. The polysilazane coating is used to reduce the shedding of CNT fibers from the sheet when the sheet is in contact with surfaces. Most fabrics show some shedding of fibers during the washing or abrasion of the fabric. This study showed that the coating reduces the shedding of fibers from CNT fabric. The coating also increased the flame resistance of the fabric. The pristine and coated sheets both have low strength but high strain to failure. The pristine and coated CNT sheet densities are 0.48 g/cc and 0.65 g/cc, respectively. The pristine CNT sheet is approximately 27 μ thick. The coated sheet is approximately 24 μ thick. The coating may have densified the sheet, making it thinner. The thickness of the compliant sheets was difficult to measure and is a source of error in the properties. Characterization results are given in this paper. The results are for comparison purposes and not to establish material properties data. Possible applications for CNT sheets are briefly discussed.

Keywords: carbon nanotube sheet; pristine; polysilazane-coated; fiber shedding



Citation: Giri, P.; Gill, I.; Swensgard, M.; Kaiser, A.; Rust, A.; Stuparyk, B.; Fisher, A.; Williams, J.; Renoit, K.; Kreeb, E.; et al. Pristine and Coated Carbon Nanotube Sheets—Characterization and Potential Applications. *C* **2024**, *10*, 17. <https://doi.org/10.3390/c10010017>

Academic Editor: Jandro L. Abot

Received: 4 December 2023

Revised: 28 December 2023

Accepted: 5 January 2024

Published: 9 February 2024



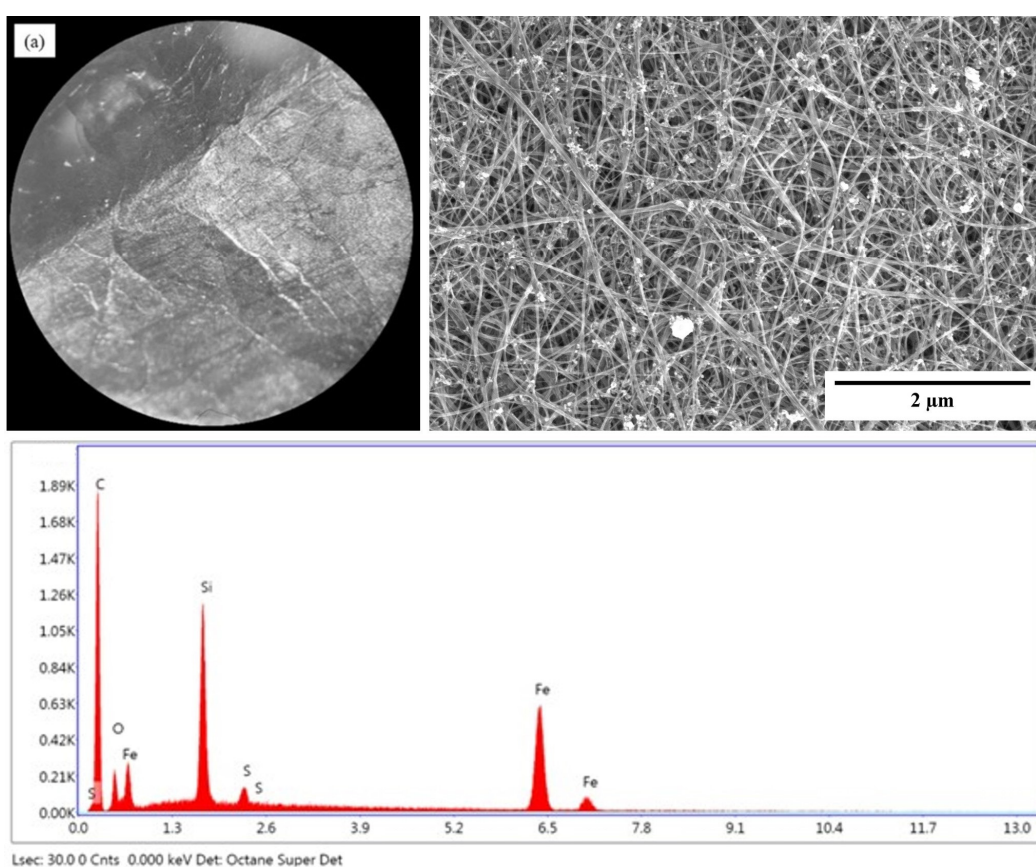
Copyright: © 2024 by the authors. Licensee MDPI, Basel, Switzerland. This article is an open access article distributed under the terms and conditions of the Creative Commons Attribution (CC BY) license (<https://creativecommons.org/licenses/by/4.0/>).

1. Background

A carbon nanotube (CNT) sheet is produced using the floating catalyst chemical vapor deposition (FCCVD) method. A CNT sheet can shed fiber strands due to contact with different surfaces and due to abrasion, such as when washing the sheet. A coating or sealant can be used to reduce shedding, e.g., silicone which was investigated in [1]. Another type of coating is a polysilazane sealant. Huntsman Advanced Materials [2] provides a commercial pristine CNT sheet called Miralon and a CNT sheet coated with a polysilazane sealant. This paper describes methods for characterizing CNT sheets and compares the properties of the pristine and polysilazane-coated CNT sheets. The following tests were performed to characterize the properties of pristine and polysilazane-surface-coated CNT sheets: (i) vertical flame test, (ii) average resistivity, (iii) tensile strength, (iv) Raman spectroscopy, (v) handleability (subjective analysis), (vi) density, and (vii) hydrophobicity. Possible applications for the sheets are also proposed in this paper. Pristine CNT sheets are described in [2,3]. The CNTs are formed in a tube reactor. Individual CNTs agglomerate into strands, and a spider-web-like sock of CNT strands exits the reactor tube. The sock is wound onto a translating and rotating drum layer by layer to form a sheet. The sheet is fluffy and is densified using a solvent such as acetone either during the synthesis process or after the sheet is formed. A pristine sheet can be coated with polysilazane. The polysilazane coating on the CNT sheet is applied in a post-processing step after the pristine sheet is manufactured. Post-processing means modifying the CNT fabric after it has been manufactured, not during the manufacturing process. Polysilazane is a high-temperature-stable, chemically resistant surface coating. The parent sheets characterized in this paper

were large (42 in × 92 in) size and manufactured for textile applications [2]. Small samples were cut from the parent sheets to perform the various tests.

The handling of pristine CNT and polysilazane-coated CNT sheets was performed using established safety protocols including wearing gloves and cleaning surfaces and fixtures to remove any debris produced from preparing and testing the samples. Images of the materials are shown in Figure 1. Per the manufacturer [2], the degree of assembly of CNT sheets with intertwined CNT strands provides structural integrity, making them functionally and mechanically different from a nanotube powder. CNT sheets are classified as articles, bulk constructions, rather than particles, a loose collection of free tubes. CNT products are not considered chemicals by the EPA and, therefore, are not subject to the same regulatory requirements. The latest safety data sheets (SDS) can be requested from the manufacturer [2]. One pertinent note from the SDS Accidental Release Conditions states the following: Avoid creating dusty conditions and prevent wind dispersal. Vacuum dust with equipment using a HEPA filter and place in a closed labeled waste container.



eZAF Smart Quant Results

Element	Weight %	Atomic %	Net Int.	Error %	Kratio	Z	R	A	F
C K	64.08	82.11	774.42	8.15	0.23	1.06	0.96	0.34	1
O K	8.82	8.48	102.17	12.29	0.01	1.01	0.98	0.15	1
Si K	6.55	3.59	652.93	4.32	0.05	0.92	1.03	0.77	1
S K	0.78	0.37	70.08	14.02	0.01	0.91	1.04	0.87	1.01
Fe K	19.78	5.45	571.70	2.76	0.16	0.78	1.08	1.02	1

Figure 1. Cont.

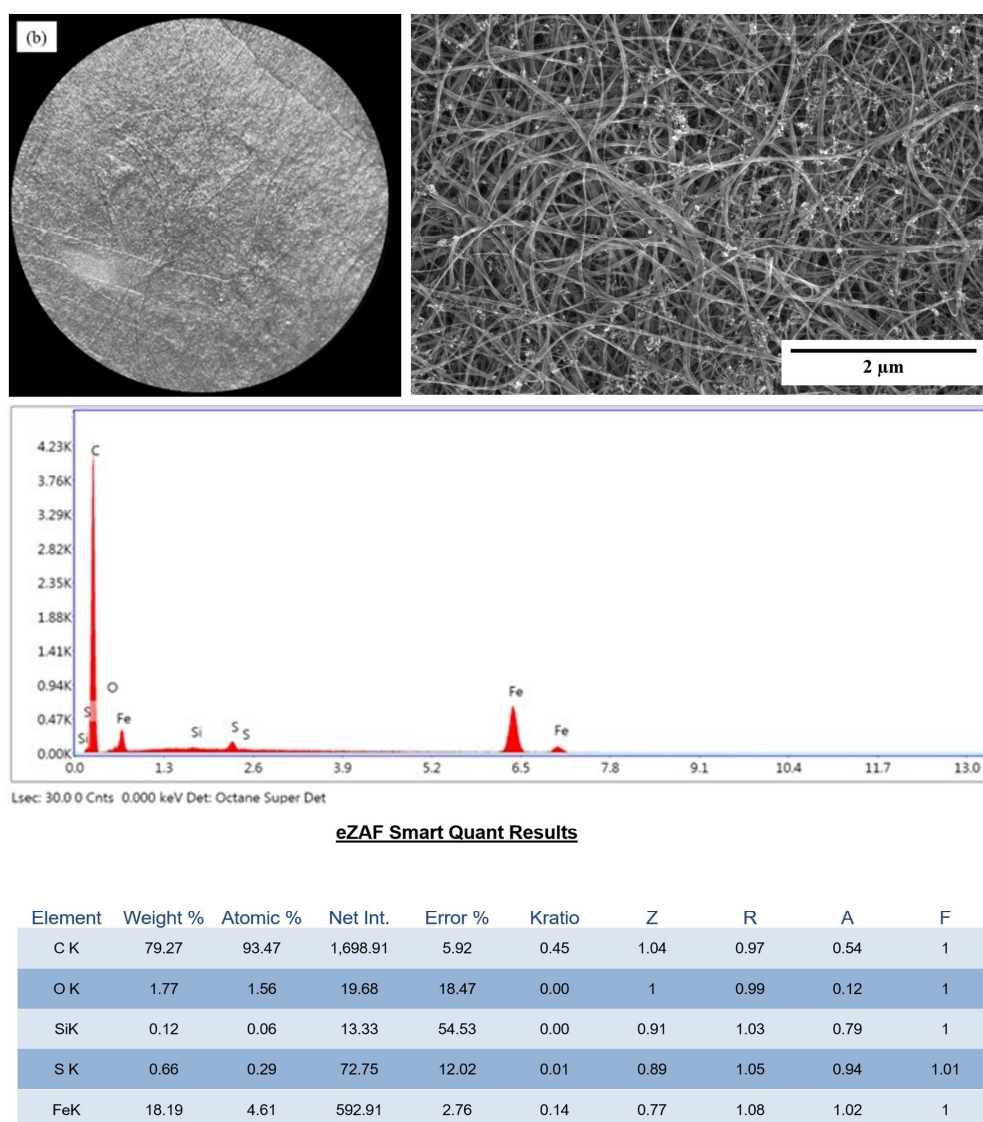


Figure 1. CNT sheet characterization. (a) Polysilazane-coated CNT sheet under an optical microscope at 15 \times . Polysilazane-coated CNT sheets have a smooth surface. Also, polysilazane-coated CNT sheet SEM image and EDAX chart are shown. (b) Pristine CNTs with the nonwoven bundles of CNTs visible at 15 \times magnification. Pristine CNT sheet SEM image and EDAX chart are also shown. The SEM is at 20,000 \times magnification.

Characterizing the polysilazane coating is discussed next. The polysilazane coating is very thin. The polysilazane CNT fabric scanning electron microscopy (SEM) image and energy dispersive X-ray analysis (EDAX) are shown in Figure 1a. The coating is not obvious in the SEM images. However, the EDAX graph for the polysilazane sample has a significant Si peak (6.55%) which the pristine sample (0.12%) does not have. The pristine CNT fabric SEM image and EDAX chart are shown in Figure 1b.

Polysilazane Sealant Description

The sealant used in this testing is a polysilazane material. One current supplier of polysilazane is Hathaway Advanced Materials [4,5]. A similar material called Durazane is available from Merck Company. This is a low-viscosity liquid. Polysilazane can be thermoset to form a solid by heating with a free radical generator or by elevated temperature. Polysilazane typically is used as a powder binder and ceramic/metal adhesive. The investigated polysilazane coating is in the form of a pre-ceramic polymer since it has not

seen temperatures needed to fully form the ceramic. It will convert when it experiences flames or high temperatures. Huntsman Advanced Materials crosslinks the coating at less than 175 °C so it is still a polymer. Polysilazane is meant to be a high-temperature-stable, chemically resistant surface coating. The material safety data sheet (MSDS) was followed for the handling of polysilazane (the as-purchased material can be flammable). But pristine CNTs and CNTs treated with polysilazane are not flammable. The specific sealant material used to coat the CNT sheets was polyureasilazane which was produced as a custom run using the exact process conditions developed for Ceraset 20, which is a discontinued material. The polyureasilazane was applied from a dilute solvent solution (3% in acetone by weight). Technical information on an equivalent material is given in [6].

The coating is applied to pristine CNT sheets in a post-processing method (after the full CNT sheet is formed) and is a surface coating applied by spraying. Other details of the process of applying the polysilazane coating to CNT sheets are company information not available for publication. The coating is an organic polysilazane. The coating works by forming dense ceramic layers with a Si–N–Si and Si–O–Si structure. The layers this coating creates are highly temperature-resistant and provide excellent protection against corrosion and weathering. They are also hydrophobic which makes cleaning surfaces easier. Polysilazane has a clear-to-hazy yellow liquid color. Its density at 25 °C is 1.0 g/cc. Its viscosity at 20 °C is 10–50 CP; turbidity is less than or equal to 10 NTU active content. Its shelf life is 18 months from production date when stored between 5–25 °C. Characterization of polysilazane curing is described in [6].

This paper gives details of the instrumentation used and testing performed to characterize CNT sheets. However, external independent testing would need to be performed in the future to qualify the materials for specific applications. Huntsman Advanced Materials recommends the same handling procedures for polysilazane-coated sheets as used with their raw or condensed sheets. Material safety data sheets [2] for CNT sheets should be read before using the sheets. Testing is described in the following sections.

2. Experimentation

Select tests were performed based on the properties that are most important to consider for different applications of CNT sheets. Thermal conductivity testing is also important but is more complex and was not performed herein. Appropriate safety protocols were followed for the tests per the MSDS for CNT sheets. For all the different tests, 5 samples of a pristine sheet and 5 samples of a polysilazane-coated sheet were tested to ensure the results were representative of the material.

2.1. Sheet Thickness Measurement

One of the challenges in characterizing thin fabrics is measuring the thickness of the fabric or sheet. Here, the sheets' thickness was initially measured using a vernier caliper (cost: USD 35), shown in Figure 2a. Using a caliper can easily lead to inaccurate readings since the material is compressible and very thin. The sheets were folded to form four layers to improve the measurement accuracy. The thicknesses of both the pristine and polysilazane-coated sheets were measured using the vernier caliper and interpolated to be about 27.5 μ . The error in this measurement was estimated to be up to 5 μ , or about 18%. To improve accuracy, the thickness of each sheet was also measured using a Hitachi TM3000 Tabletop Microscope (cost: USD 76,000). Three samples of each sheet were measured using the benchtop SEM with an acceleration voltage of 5 kV to determine the average thickness of the sheets. The average thickness of the pristine sheet was 27.3 microns with a standard deviation of 1.08 microns (Figure 3a). The average thickness of the polysilazane-coated sheet was 24.14 microns with a standard deviation of 0.66 microns (Figure 3b).



Figure 2. Instruments for measuring the size of the sheets. (a) Vernier caliper, where force on the adjustment wheel changes the thickness reading, using multiple folds of fabric to increase accuracy of measurement, versus the (b) Hitachi TM3000 Tabletop scanning electron microscope (SEM).

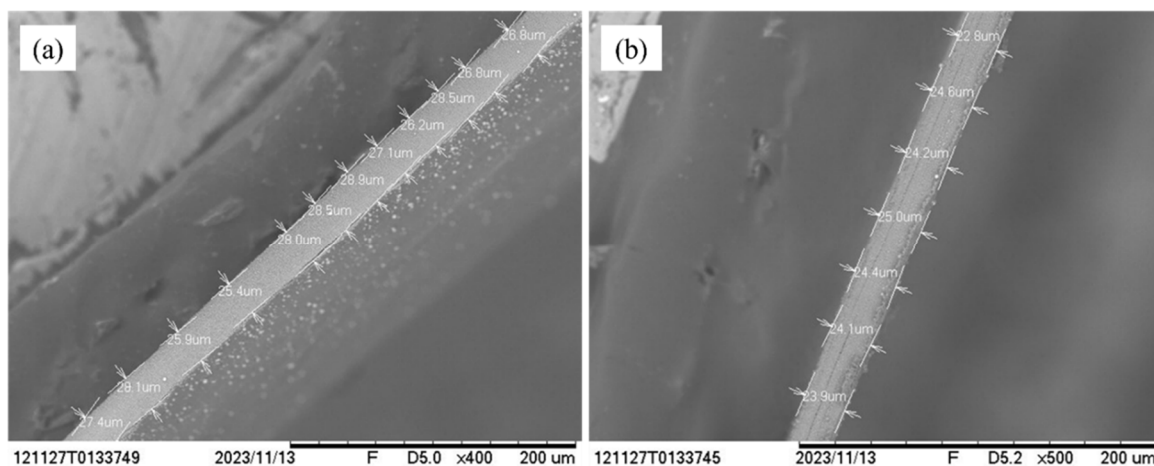


Figure 3. Measuring the thickness of CNT sheet using a benchtop electron microscope. (a) The average thickness of the pristine CNT sheet was 27.3 μ . (b) The average thickness of the polysilazane-coated CNT sheet was 24.1 μ .

Solvent in the polysilazane coating evaporates and may have densified the CNT sheet further which could have decreased the thickness of the sheet compared to the uncoated pristine sheet. The thickness values measured using the tabletop SEM were used for calculating the density, strength, and electrical resistivity of all of the samples used in testing. It was assumed that the large CNT sheets have uniform thickness.

2.2. Vertical Flame Test

2.2.1. General Procedure

The general procedure followed for the test is as follows: (i) place the sample vertically in the setup, (ii) light the torch to a suitable flame length (~ 38 mm), (iii) put the torch ~ 19 mm below the sample for 12 s, (iv) remove the torch and measure the after-flame time, afterglow time, and char length. The vertical flame test was performed to check the compatibility of the sheets with standard ASTM D6413. The test was performed inside a fume hood with necessary equipment. The samples were held vertically in a stand. A propane torch was used to generate a flame with suitable length. The tip of the propane torch head was placed by hand so that the sheets were exposed to the proper zone of the flame.

2.2.2. Experimental Results

Figure 4 shows the setup employed for the vertical flame test, ensuring secure fixation of the sample. The sheets were subjected to 12 s of direct flame from a propane torch. The polysilazane-coated CNT sheet exhibited a delayed ignition response. The pristine CNT sheet displayed a comparatively swifter ignition response. Furthermore, our examination noted a significant reduction in flame propagation along the polysilazane-coated CNT sheet, with the flame extinguishing relatively swiftly as it ascended the material. The pristine CNT sheet exhibited similar behavior, but with a longer char length. This observation is corroborated by the determination of tear length, where the polysilazane-coated CNT sheet exhibited a tear length of 11 mm, whereas the pristine CNT sheet demonstrated a tear length of 20 mm, after the material underwent the flame test. The shorter tear length indicates less damage from the flame. CNT sheets have good thermal conductivity. Spreading heat away from the flame area may have reduced the temperature of the sheets which could have extended the time required for the sheet to be damaged.

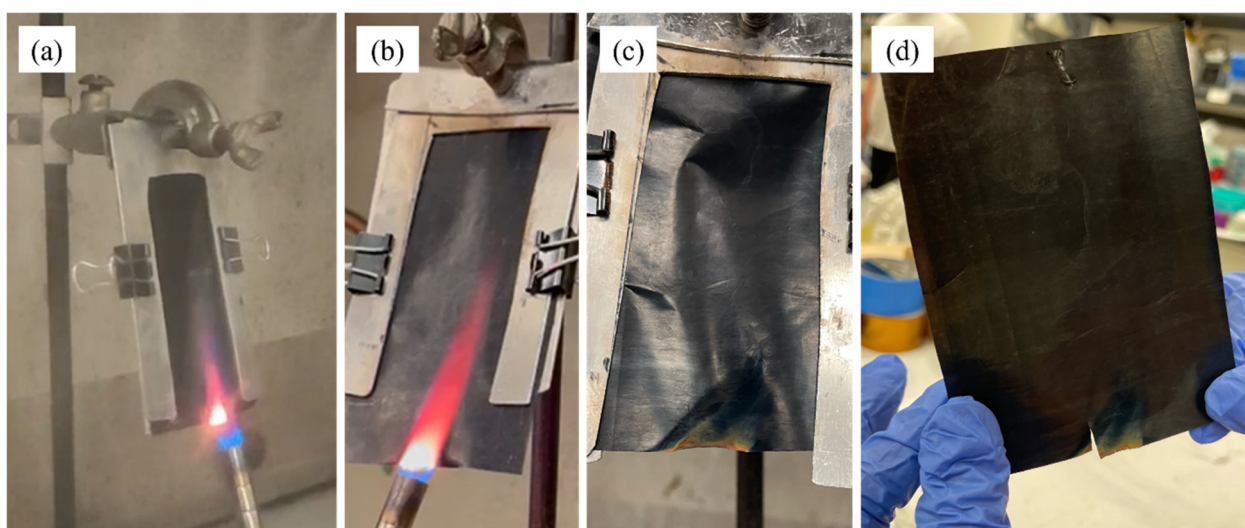


Figure 4. Flame testing polysilazane samples. (a,b) Flame applied to two samples. (c) Sample after flame was removed. (d) 11 mm tear in polysilazane-coated sample after flame testing.

During this experiment, samples were placed into an aluminum frame the same way for the pristine and polysilazane-coated samples. The human reaction time to starting and stopping the flame test and positioning the flame could have caused error in this experiment. Five different samples of the pristine sheet and five different samples of the polysilazane-coated sheet were tested and qualitatively produced repeatable results. Overall, these findings provide crucial insights into the flame resistance and behavior of polysilazane-coated CNT and pristine CNT sheets. This testing indicates that CNT sheets might be used in applications needing fire-resistant properties such as firefighter garments. After-flame time, afterglow time, and char length were measured and are given in Table 1.

Table 1. Results of the vertical flame test.

Sample	After-Flame Time	Afterglow Time	Char Length	Tear Length
Pristine CNT	<1 s	<1 s	<30 mm	20 mm
Polysilazane-coated CNT	<1 s	<1 s	<30 mm	11 mm

The polysilazane coating offers better flame resistance, preventing the CNT sheet from igniting easily. The absence of sparks or release of burning particles suggest that the polysilazane coating acts as a barrier, reducing direct exposure of the CNT sheet to the flame

which reduces the rate of combustion. CNT will decompose in an oxidative environment before reaching 900 °C. The oxidation product of carbonaceous materials is CO₂ which is not flammable; see [7]. Residual orange oxidized iron catalyst also appears on the sheet due to the flame test. Iron catalyst is used to synthesize the CNT sheet. In addition, the reduced char length in the polysilazane-coated sample indicates its superior thermal stability and resistance to degradation at elevated temperatures compared with pristine CNT fabric. It is also possible that the polysilazane coating contains certain chemical components that interfere with the combustion process, leading to less char formation. Overall, coating or sealing CNT sheets with different materials can be customized for different applications.

A commercial material that CNT fabric may be compared to is nonwoven meta-aramid (Nomex[®]) [8]. Nomex is electrically insulating and stronger than CNT fabric and operates up to 230° C. Polysilazane-coated CNT can operate at higher temperature and is electrically conductive [8]. The results in Table 1 are presented to show compliance with the vertical flame test of fabrics. The after-flame time, afterglow time, and the char length complied with the ASTM D6413 vertical flame test (the char length was less than 6 inches and no melting or dripping of the samples was observed). The ASTM standard is itself taken as a benchmark for developing various high-temperature equipment, such as personal protective equipment (PPE) for firefighters. Since other fabrics are very different than CNT fabrics, we presented a comparison of two types of CNT sheets, so that a selection based on their properties can be made when a need for such materials arises. For example, one may select pristine CNT when larger strain is desired, whereas polysilazane-coated CNT may be useful when higher flame resistance and an isotropic nature are required.

2.3. Average Resistivity of Thin CNT Sheets

2.3.1. General Procedure

A Delcom Instruments device was used in this experiment to measure sheet resistance using eddy currents. Sheet resistance was created as a unit of measurement for thin-film materials. Sheet resistance is a measure of the electrical properties of a material independent of the in-plane dimensions. Eddy current meters can measure sheet resistance, thickness, and resistivity. Four-point probes are the traditional instruments for determining electrical resistance. Two articles cover the measurement of electrical and thermal properties of thin and thick films [9,10]. Sheet resistance (units ohm/sq) was measured based on an eddy current formed in the plane of the CNT sheet. Thin-film resistivity is computed by multiplying the sheet resistance by the thickness (units ohm*cm). The Delcom eddy current meter is nondestructive, reads through insulating layers, measures moving material, provides nearly instantaneous readings, provides real-time process inspection and quality control, provides better repeatability than contact methods, and is lower cost than using four-point probes.

The general procedure followed for the test is as follows: (i) set the measurement device on a flat surface away from magnetic fields; (ii) place the sample and record the readings at different places and take an average. Average sheet resistance gives us a comparison of resistance of all the samples in an arbitrary unit Ω/sq. The values can be multiplied by the thickness of the samples to obtain the thin-film resistivity. Note that CNT sheets have anisotropic electrical conductivity, and the sheet resistance measurement gives a representation of the resistivity at a point. The resistivity through the thickness of CNT fabric is much greater than the resistivity in the plane of the fabric because the millions upon millions of CNT strands that are intermingled represent junctions with high resistance. There are more junctions through the thickness of the fabric than in-plane, per unit length. The resistivity of the fabric can also vary between the winding direction and perpendicular to the winding direction in-plane. The resistivity in the winding direction can be lower than in the perpendicular direction. The thin-film electrical resistivity in ohm cm is the most important sheet parameter used in electrical design.

2.3.2. Experimental Results

The average sheet resistance was measured for polysilazane-coated CNT and pristine CNT using the Delcom eddy current meter (Figure 5). Five different samples of a pristine sheet and five different samples of a polysilazane-coated sheet were tested and showed consistent measurements of sheet resistance. Then, the sheet resistance was measured at 12 places for one pristine sheet and 12 places for one polysilazane-coated sheet. The average sheet resistance of the pristine CNT sheet was $0.6491 \Omega/\text{sq}$. with a standard deviation of $0.0185 \Omega/\text{sq}$. The average sheet resistance of the polysilazane-coated sheet was $0.4820 \Omega/\text{sq}$. with a standard deviation of $0.01 \Omega/\text{sq}$. The average resistivity for the two sheets was then calculated. The sheet resistance was multiplied by the thickness to obtain resistivity. The calculations are below.

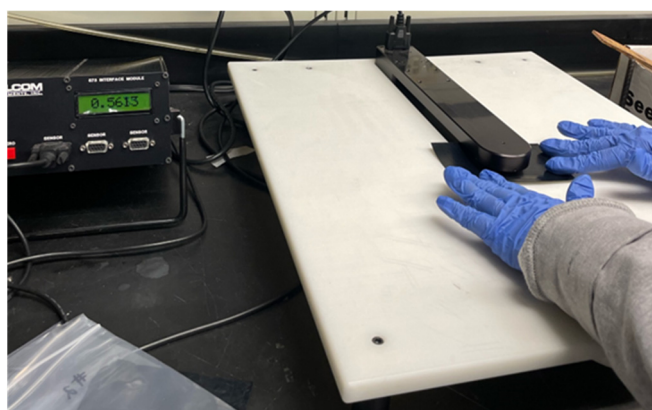


Figure 5. Measuring electrical sheet resistance of CNT sheet using a non-contact eddy current meter.

Pristine CNT sheet resistance measurements are: 0.6523, 0.6412, 0.6463, 0.6423, 0.6809, 0.6446, 0.6732, 0.6703, 0.6529, 0.6093, 0.6315, and 0.6444 ohm/sq. The average of the values is 0.6491 ohm/sq . The thin-film resistivity = $0.6491 \times 0.00273 = 0.001772 \Omega \text{ cm}$.

Polysilazane-coated CNT sheet resistance measurements are: 0.4742, 0.4621, 0.4744, 0.4825, 0.4890, 0.5006, 0.4946, 0.4813, 0.4819, 0.4775, 0.4892, and 0.4764 ohm/sq. The average of the values is 0.4820 ohm/sq . The thin-film resistivity = $0.4820 \times 0.002414 = 0.001164 \Omega \text{ cm}$.

The resistivity values are summarized in Table 2. The lower resistivity of the polysilazane-coated CNT sheet may have resulted from compaction in the sheet thickness that occurred during the coating process, which might have improved the contact between nanotube junctions. Both pristine and polysilazane-coated CNT have electrical resistivity in a range between polymers and metals. Polysilazane has a slightly lower resistivity. The thin-film resistivity characterizes the resistance to electrical current flow within the plane of the material. Since the polysilazane-coated CNT sample had a lower thickness than the pristine sample, the resistivity of the polysilazane-coated CNT sample is lower than that of the pristine sample. It should be noted that an error of 18% is possible in the resistivity measurements due to error in measuring the thickness of the compressible CNT fabrics.

Table 2. CNT sample electrical measurements.

S. No.	Sample Name	Average Sheet Resistance (Ω/sq)	Thickness (cm)	Thin-Film Resistivity ($\Omega \cdot \text{cm}$)
1	Pristine CNT	0.649	0.00273	0.0018
2	Polysilazane-Coated CNT	0.482	0.00241	0.0012

Both CNT samples have a low sheet resistance, especially compared to typical textiles, like cotton. Pristine cotton fabrics have an extremely high electrical sheet resistance ($\sim 10^9 \Omega/\text{sq}$) [11]. The standard AATCC 76-2000 Electrical Surface Resistivity of Fabrics describes methods for the measurement of surface resistivity of woven fabrics. This test

method is applicable for resistivity measurements generally above $10^7 \Omega/\text{square}$. CNT fabric is, thus, unique for applications requiring conductive textiles.

2.4. Tensile Strength

2.4.1. Procedure

The procedure is as follows: (i) prepare the samples, being careful to not damage the edges (contactless laser cutting is used); damage on the edge can act as a stress concentration and become a failure point; (ii) mount the samples on a paper frame; (iii) perform the tensile test with recommended settings for the load range needed to break the CNT samples. Stress–strain graphs were prepared using the Instron tensile test machine. Thin strips of CNT fabric were laser cut from large sheets for testing. The Oxford Lasers Micro Machining System is shown in Figure 6a. It cut the CNT fabric to a rectangle at a rate of 4 mm/s (Figure 6b). Note it is important to center the CNT fabric with respect to the machine's X, Y, and Z axes. Preparing the paper frame used as a fixture for holding the CNT specimen is shown in Figure 6c. The Instron tensile test machine is shown in Figure 6d.

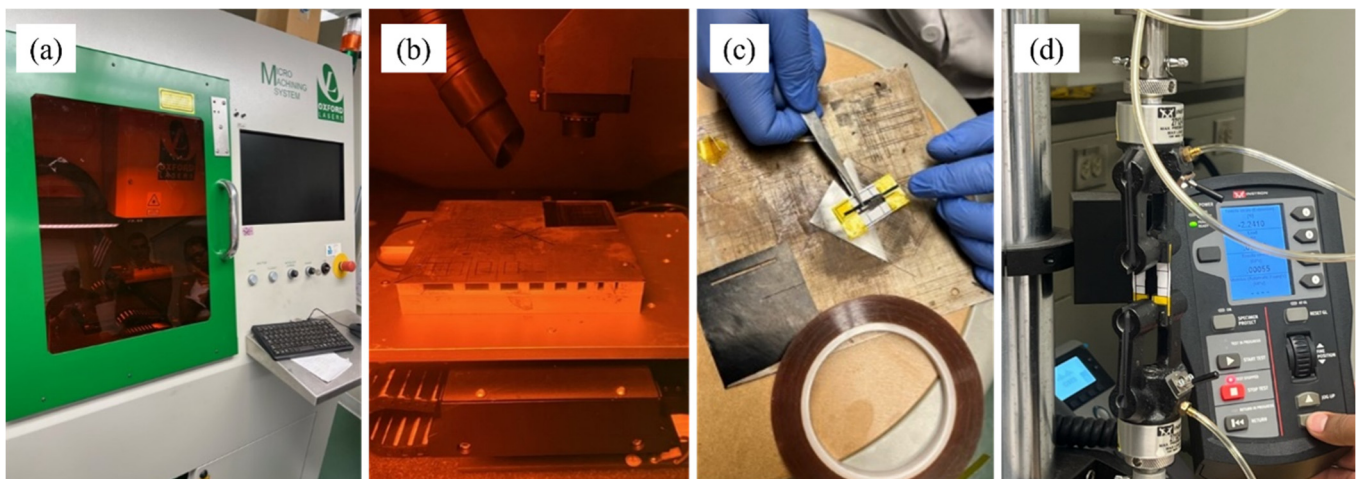


Figure 6. Preparing the CNT samples for tensile testing. (a) Oxford Lasers Micro Machining System. (b) Laser cutting of CNT sheet sample. (c) Paper frame is used to support the CNT tensile specimen just for mounting into the tensile test machine. The paper is cut after the sample is mounted into the Instron machine. (d) Benchtop Instron tensile test machine for measuring the strength of small-sized samples. The Instron machine is Model 5948.

The Instron tensile test machine measured the strain and resulting stress in the CNT test specimens. The purpose of using the laser is to make precise cuts of CNT specimens to test tensile strength without the inclusion of a micro-tear (i.e., crack). Micro-tears reduce the ultimate tensile strength of the fabric because they act as a stress intensity factor. A CNT sheet with a tear (i.e., crack) that is perpendicular to the force being applied takes lower force to tear than if it were not damaged. It is crucial to use a fixture to ensure the load is applied in the tensile direction and no off-center load is applied. Paper frames acted as a fixture to ensure the CNT specimens were loaded perpendicular to the arms of the Instron machine. Otherwise, the measured tensile strength of CNT specimens would significantly decrease as the Instron would be applying a tensile and shear load on the CNT specimen. It is worth noting that the tensile strength of paper fixture is not relevant as the paper was cut after placing the fixture in the Instron machine.

2.4.2. Experimental Results

Pneumatic grips were used to hold the samples for the test. Five samples, each along the length and width directions of the large sheet, were prepared for both pristine CNT and polysilazane-coated CNT sheets. The length/width directions are denoted as D1/D2

and sample numbers are denoted as S1, S2, S3, S4, and S5. Twenty CNT sheet specimens (ten pristine, ten polysilazane coated) in total were used for this test. The samples were cut to a nominal length of 20 mm and a width of 2 mm within laser-cut tolerances in each of the two directions (perpendicular to each other). Both the pristine and polysilazane-coated CNT samples were prepared using a laser which was programmed to make four passes to ensure that there was minimal fraying along the edges of the samples. This led to four sets of five CNT sheet combinations of type and cut direction. Thus, five samples were prepared in one direction and then five more samples were prepared 90° from the original samples. Figure 6d shows the Instron machine with the sample mounted. It was strain-controlled to a rate of 1 mm/min. The results of this test should be used for relative comparison of the pristine and polysilazane-coated materials. The CNT fabric's failure looks like a tear across the fabric in the perpendicular direction to the load applied. Stress–strain plots are shown in Figures 7 and 8.

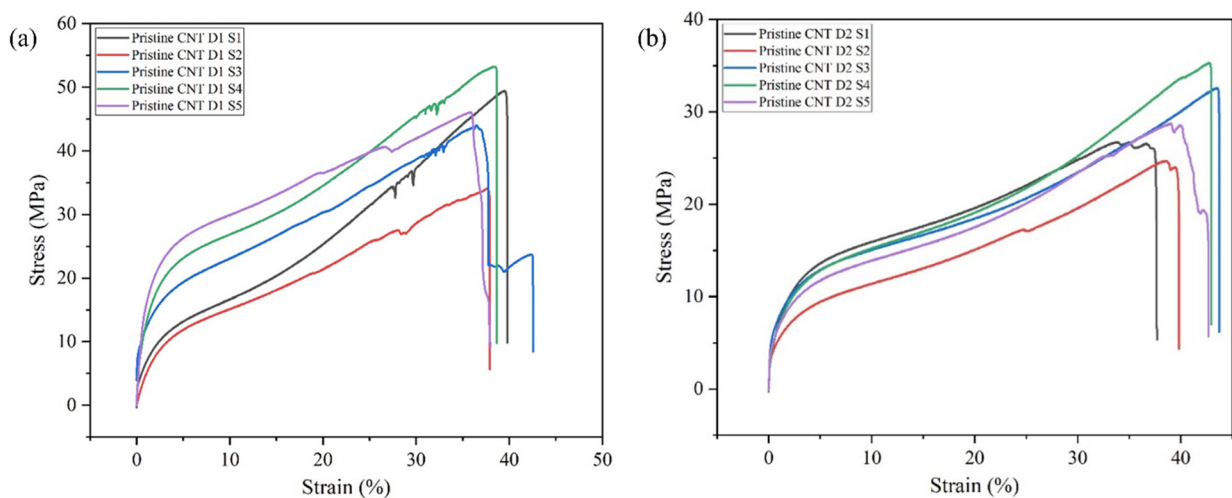


Figure 7. Pristine CNT sample testing. (a) Along direction D1. (b) Along direction D2.

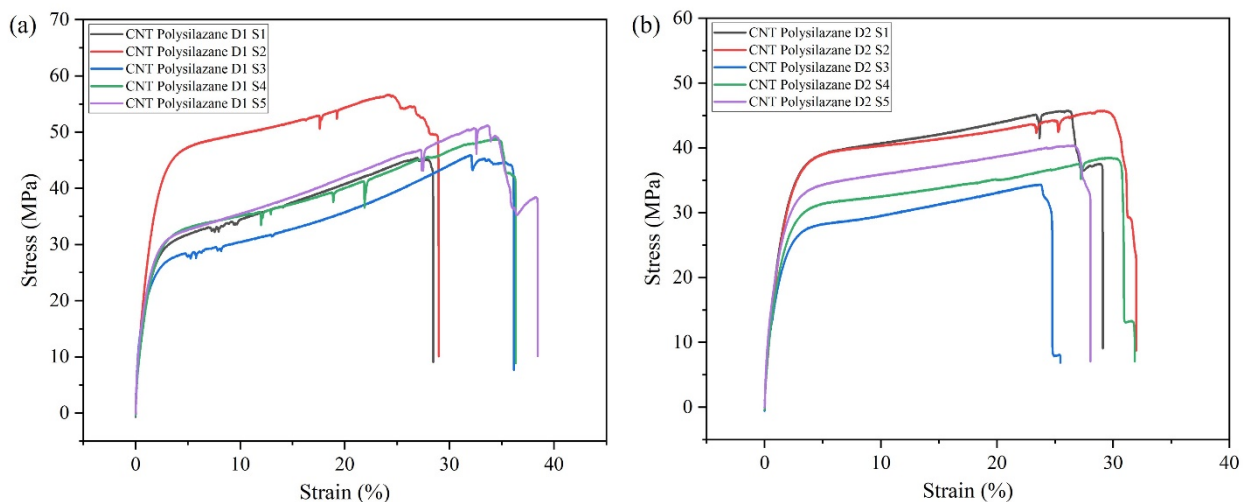


Figure 8. Polysilazane-coated CNT sample testing. (a) Along direction D1. (b) Along direction D2.

The ultimate strength was used for calculations. The average ultimate strength of the pristine sheet along its length (D1 direction) was 45.6 MPa with a standard deviation of 6.5 MPa. The same average across its width (D2 direction) was 29.9 MPa with a standard deviation of 3.99 MPa. Similarly, the average ultimate strength and standard deviation of the polysilazane-coated sheet along its length (D1 direction) were 49.4 MPa and 4.22 MPa,

respectively. The same average and standard deviation across its width (D2 direction) were 41.2 MPa and 4.35 MPa, respectively.

The strain at failure of the pristine fabric was approximately 39/42% in the D1/D2 directions. The strain of the polysilazane-coated CNT fabric was approximately 35/30% in the D1/D2 directions. Visually, the polysilazane-coated CNT sheet had a greater yield strength and greater slope (elastic modulus) than the pristine CNT sheet. The increased stiffness of the polysilazane-coated sheet versus the pristine sheet is attributed to the polysilazane bonding to the CNT strands in the sheet and to the polysilazane coating itself cross-linking around the CNT strands. Regarding the polysilazane-coated CNT sheet's stress–strain plot, the slope from 0 to ~30 MPa is steep and linear then tapers off to almost a flat line from ~30 MPa to the average failure of ~49 MPa. The same trend is seen in direction 2 (D2). This indicates that the polysilazane coating increased the tensile modulus of the CNT sheets. The strain to failure is greater in the pristine CNT sheet than in the polysilazane-coated CNT sheet. This is likely because the polysilazane bonds the CNT bundles together and when the fabric fails, the bonds are more brittle and break whereas the pristine CNT sheet fails by the CNT bundles sliding apart, overcoming the van der Waals forces.

Another observation is the large variation in the stress–strain curves. This is attributed to sample preparation (alignment of the sample in the Instron machine and cutting the CNT sheets using the laser) and due to possible variations in thickness of the CNT sheets and polysilazane coating. Overall, the testing shows that CNT fabric, being nonwoven, has low strength but very high strain to failure in the plane of the fabric. Future work would be to test CNT fabric while considering thickness in compression to ascertain what applications may benefit from using the material in compression. Thicker sheets would be needed for compression testing.

Pristine CNT sheets that contact surfaces or other fabrics can shed fiber particles or strands onto said surfaces. Various coatings were considered to reduce the shedding of CNT strands. Polysilazane was selected because of its low viscosity and because it can be applied easily by post-processing. Also, there are more compacted CNT strands in the polysilazane-coated sheet versus the pristine sheet. Thus, the greater load transfer through the CNT strands in the polysilazane-coated CNT sheet is an added advantage.

The strengths are different in directions D1 and D2 because of the direction of CNT fiber strands that were pulled out of the furnace and wrapped on the take-up drum. For example, along the direction that the CNT fiber strands were pulled can be thought of as along the grain, and strength of a material along its grain (or length) is greater than along the perpendicular direction, which is shown in woodworking. Some samples showed kinks in the stress–strain curves. These are attributed to edge defects in the samples due to laser cutting.

2.5. Raman Spectroscopy

2.5.1. Procedure

Raman spectroscopy is used herein to indirectly measure the quality of CNT sheets. Raman spectroscopy is sensitive to highly symmetric covalent bonds with little or no natural dipole moment [12]. The C–C bonds that form the CNTs fit this criterion. Thus, Raman spectroscopy provides information about CNT structure. The Raman effect is based on the change in the wavelength of light. The change occurs when light is redirected by molecules. The interaction between the photons and the chemical bonds in a material changes the wavelength of the light. When light travels through a material, part of the light is scattered, and a small part of the scattered light has a change in wavelength. When photons hit molecules, most of the interactions are elastic. Thus, the energy and frequency of the photons remains the same. However, sometimes the molecule transfers energy to or takes energy from the photon. The change in energy of the photon causes a change in frequency. The frequency shift is a measure of the change in energy. The energy is associated with changes in different rotational and vibrational modes of the molecule.

The procedure for testing is as follows: (i) power on the Raman instrument with recommended settings; (ii) place the sample and focus the beam and laser; (iii) collect Raman spectrum.

A high-intensity laser is used as a light source with a known wavelength. The Raman instrument, Figure 9a, measures the changes and wavelengths and outputs a Raman spectrum showing the intensity of the Raman scattered light at different wavelengths. The wavelength peaks correspond to specific molecular bond vibrations and different groups of bonds. As a note, because the instrument relies on vibrations and accurate reading of the scattered laser, even small movements of the table and machine may lead to error.

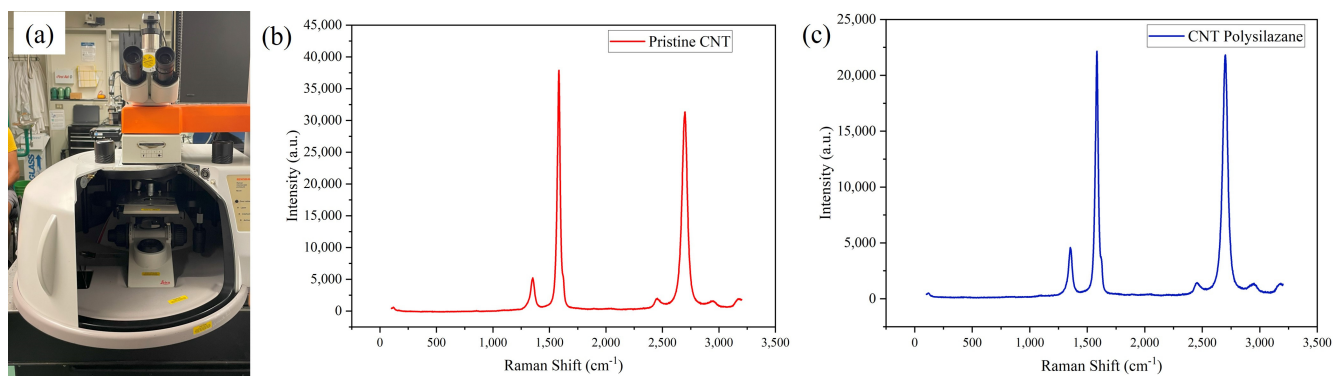


Figure 9. Raman graphs. (a) Raman spectrometer. (b) Pristine CNT plot. (c) Polysilazane-coated CNT plot.

Typically, the Raman spectrum of CNT contains a “G” band around 1580 cm⁻¹, a “D” band around 1300 cm⁻¹, and a “2D” band at around 2600 cm⁻¹. Here, we are mainly concerned about the G and D bands. The G band is associated with the specific bonds of the carbon atoms in the CNT, the D band is a result of defects in the CNT, and the 2D band is a resonant peak occurring as an overtone of the D band. The intensity ratio of the G band to the D band indicates the quality of the CNT. The Renishaw inVia Raman spectroscopy instrument with a 514 nm wavelength was used to analyze the CNT-based materials. A laser spot size of ~1 μm² and a lens of 50× magnification was used for this study. The exposure time (10 s) and the number of accumulations (3) were kept the same for both the pristine CNT and polysilazane-coated CNT samples.

2.5.2. Experimental Results

The Raman instrument and plots, Figure 9b,c, were generated from an average of three measurements at a single location on the sample sheet. In the pristine sample’s Raman spectrum, Figure 9b, the intensity at the G band was about 37,500, while the intensity at the D band was 5000. In the polysilazane-coated sample’s Raman spectrum, Figure 9c, the intensity at the G band was about 22,500, while the intensity at the D band was 5000. The G/D ratio of the peaks for the pristine CNT sample is 7.5 and that for the polysilazane-coated CNT sheet is 4.5. The ratio for the pristine sample is higher, which means that it is higher quality and has fewer defects than the polysilazane-coated CNT.

Reference [13] states: “Raman spectroscopy provides a semiquantitative indication of purity or degree of functionalization by comparing the relative intensity of the defect band (D-band) at ~1350 cm⁻¹ and the graphite band (G-band) at ~1580 cm⁻¹; although the details are complex, increasing D-band intensity is usually correlated with either the presence of other contaminating carbons or damage to the nanotube framework”. Therefore, the polysilazane coating might affect the nanotube framework, causing a reduction in the G/D ratio. To determine exactly how the coating affects the nanotubes would require further study. The pristine samples with a higher G/D (graphitic/disorder) ratio indicate increased crystallinity and purity (which is related to the quality) of the CNT sheets. The polysilazane coating reduced the G/D ratio (mainly the highest peak, G, at a Raman shift of ~1600 cm⁻¹).

The G/D ratio is also influenced by the CNT manufacturing process. By reducing the fuel-to-gas ratio in the synthesis process, CNT sheets can be produced with higher purity, therefore producing higher-quality products. The CNTs are formed in a tube reactor. Individual CNTs agglomerate into strands and a spider-web-like sock of CNT strands exits the reactor tube. The sock is wound onto a translating drum layer by layer to form a sheet. The sheet is fluffy and is densified using a solvent such as acetone either during the synthesis process or after the sheet is formed. However, there is a tradeoff with quality and yield; reducing the fuel-to-carrier gas ratio produces a higher-quality and more expensive CNT sheets but at a lower yield. The G/D ratios (and all the results) reported here correspond to specific synthesis conditions and the specific reactor design. Varying the synthesis parameters (such as the fuel/gas ratio) can increase or decrease the G/D ratio and the corresponding CNT yield of the process.

In interpreting the Raman spectrum, the G band corresponds to the scattering, in the first order, from carbon atoms of atomic subdivision SP². The D band represents the peak produced by the disorder of the structure and is usually found at a lower frequency compared to the G band. Typically, materials with light atoms and strong bonds have high Raman shifts whereas heavy atoms and weak bonds have low Raman shifts. This difference is represented in the G/D ratio. The polysilazane coating reduces the G/D ratio. But further study would be needed to explain exactly how the coating affects the G/D ratio. The Raman instrument was mounted on an isolation table to prevent parasitic vibrations from interrupting the experiment.

Sources of error for Raman spectroscopy are as follows: (i) The CNT sheet is on a glass slide which may have impurities. It is better to use a metal sheet instead of glass as metal does not interact with the laser and does not cause strange counts. Using glass slides with polymers may affect the Raman value. (ii) Another source of error is human error in focusing the laser. (iii) Shaking the air table affects the focus of the glass sample so that the laser cannot measure the peaks as precisely.

2.6. Handleability (*Ability to Be Manipulated, Folded, Pulled*)

2.6.1. Procedure

Samples were handled with hands and subjective measurements of feeling/texture and sounds produced were noted. Gloves were worn.

2.6.2. Experimental Results

Figure 10a,b shows the samples examined. In this section of the experiment, we conducted a structural analysis of pristine CNT and polysilazane-coated CNT using optical microscopy and our three senses: touch, sound, and sight. These observations were carried out with the aim of characterizing their respective physical properties. When tactically examining the materials, the polysilazane-coated CNT displayed a distinct lack of rigidity, and its tactile properties closely resembled those of wax paper. Conversely, the pristine CNT exhibited even greater flexibility and presented numerous wrinkles and creases across its surface. The pristine CNT material's tactile qualities were akin to that of a typical plastic trash bag. Furthermore, during our tactile evaluation, it was noted that the pristine CNT material emitted notably less sound when manipulated compared to the polysilazane-coated CNT. These observations offer valuable insights into the physical characteristics of these materials and contribute to our understanding of their suitability for various applications.

The polysilazane-coated sample was more pleasant to the touch, while the pristine sample was much rougher. The polysilazane-coated sample is more uniform while the pristine sample has a more irregular and less homogeneous surface structure. No shedding or release of particles was observed in the handling and bending of either sample. Shedding was also tested by pressing the pristine and polysilazane-coated sheets against surfaces. Figure 10c,d shows that the pristine CNT leaves black fabric debris on a surface but the polysilazane-coated CNT mostly does not. The polysilazane-coated CNT sheet was felt to

have better handleability characteristics. It did not stick to surfaces like pristine CNT and the sample was easy to prepare, transfer, and mount.

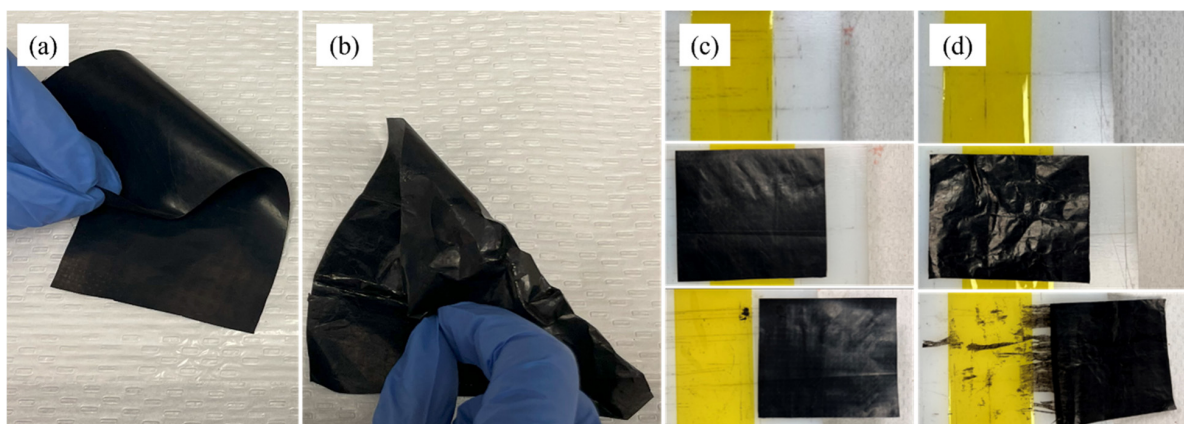


Figure 10. CNT samples handling testing. (a) Polysilazane-coated CNT sheet's folding action. (b) Pristine sheet's folding action. (c) Surface after polysilazane-coated CNT contact on scotch tape, showing release of fibers only in one location which is roughly 1% of the area of the CNT fabric. (d) Surface after pristine CNT contact on scotch tape, showing release of fibers in 14 locations which is roughly 14% of the area of the CNT fabric.

2.7. Density

2.7.1. Procedure

The experimental procedure is as follows: (i) measure the length, width, and thickness of the sample using a ruler and vernier caliper; (ii) calculate the volume; (iii) weigh the sample; (iv) calculate the density. CNT fabric is soft and compressible; thus, measuring the thickness is difficult. The thickness of CNT sheets with polysilazane-infiltrated pores sheet may decrease. This is because the polysilazane evaporates, and it may densify the sheet (due to capillarity forces during evaporation) and make the sheet thinner than the pristine sheet. This is a hypothesis about the polysilazane sheet becoming thinner. Polysilazane may also stiffen the sheet, so the thickness appears greater when measured using a vernier caliper as compared to a pristine CNT sheet which is softer. CNT sheet thickness was also measured using a benchtop scanning electron microscope (SEM) and the thickness from the SEM was used in the density calculation. The samples for density measurement were the same planar size (Figure 11).

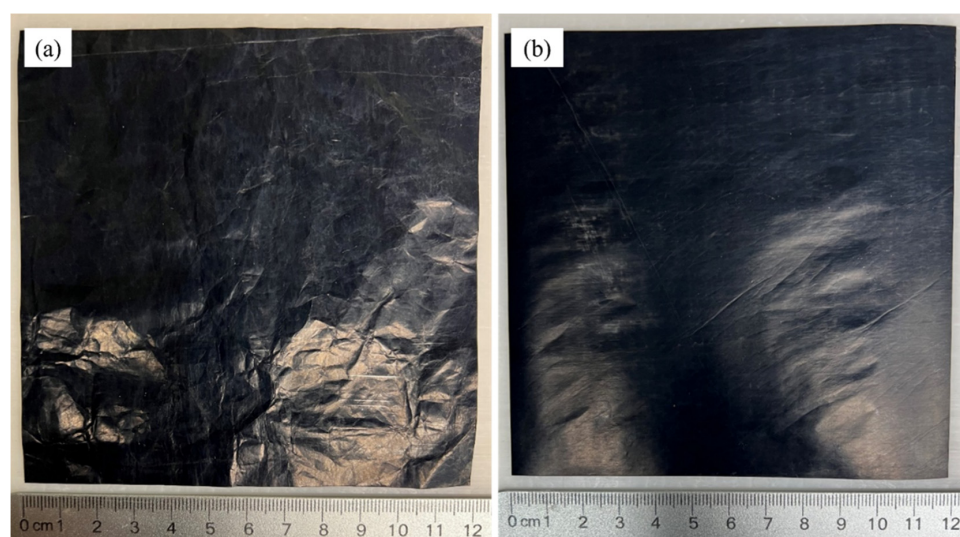


Figure 11. CNT sheet samples used for density measurement. (a) Pristine. (b) Polysilazane-coated.

2.7.2. Experimental Results

In this section, the density of each material was determined. The length, width, and thickness of each sample was measured. There could have been random error if the vernier caliper was not closed with the same pressure, as the fabric was compressible and very thin. The measurements for these three dimensions were taken multiple times. The benchtop SEM was finally used to obtain the most accurate thickness measurement. Results are listed in Table 3. Both polysilazane-coated CNT and pristine CNT exhibit exceptionally lightweight properties, boasting a minimal density that holds significant promise for various applications where weight considerations are important. Light weight enhances the overall efficiency and performance of structures and opens doors to innovative solutions in industries where minimizing weight is a critical factor. From aerospace components and automotive engineering to advanced structural materials, garments, and consumer products, lightweight properties make CNT sheets attractive.

Table 3. Density experimental results.

Type	Mass (g)	Length (cm)	Width (cm)	Thickness (cm)	Volume (cm ³)	Density (g/cc)
Pristine CNT	0.1901	12	12	0.00273	0.3931	0.48
Polysilazane-coated CNT	0.2245	12	12	0.00241	0.3470	0.65

The calculations of density are shown next. Pristine CNT and polysilazane-coated CNT samples were cut into square shapes of 12 cm × 12 cm (Figure 11). The average mass of pristine CNT sheets was 190.12 mg. The average mass of polysilazane-coated CNT sheets was 224.5 mg. The density of pristine CNT = $190.12 \times 10^{-3} \text{ g} / (12 \text{ cm} \times 12 \text{ cm} \times 2.73 \times 10^{-3} \text{ cm}) = 0.484 \text{ g/cc}$. The density of polysilazane-coated CNT = $224.5 \times 10^{-3} \text{ g} / (12 \text{ cm} \times 12 \text{ cm} \times 2.41 \times 10^{-3} \text{ cm}) = 0.647 \text{ g/cc}$. The use of polysilazane coating may have filled the voids and caused contraction in the pristine sheet, thus making the sheet denser.

2.8. Hydrophobicity Test

2.8.1. Procedure

The testing procedure is as follows: (i) place a water droplet on the CNT sheets; (ii) observe if the water spreads; (iii) place an oil droplet on the CNT sheets; (iv) observe if the oil spreads. The hydrophobicity test was performed by laying the samples on a smooth Teflon block. A drop of water was carefully dropped on top of the pristine CNT sheet and the polysilazane-coated CNT sheet and the interaction with the sheets was observed. A similar test was also conducted with oil drops to observe the oleophilic behavior of CNT sheets.

2.8.2. Experimental Results

Figure 12 shows the hydrophobicity testing samples. Both the polysilazane-coated and pristine CNT fabric demonstrated surface-level hydrophobic behavior toward the two water droplets applied to each. The polysilazane-coated CNT fabric had less water spreading than the pristine fabric; this is shown by the water droplets looking more spherical on the polysilazane-coated CNT fabric, whereas the water droplets on the pristine CNT fabric formed a slightly larger bead (Figure 12a,c). Thus, the polysilazane-coated CNT fabric is more hydrophobic than the pristine CNT fabric. When the CNT fabrics were agitated by hand (shaking the fabric), the water droplets on the polysilazane-coated CNT fabric panned out less than on the pristine CNT fabric, further demonstrating the polysilazane coating's hydrophobic properties.

When oil was applied to the polysilazane-coated and pristine CNT sheets, both demonstrated a similar behavior of the oil droplets panning out into a flat wet spot (Figure 12b,d). This is presumably because oil has lower surface tension than water, so it is easier for oil to pan out. For water and oil, once panned out on polysilazane-coated and pristine CNT

fabric, the water and oil seemed to follow the ridges/wrinkles/crevices of the fabric sheets. The backsides of the polysilazane-coated and pristine CNT fabric sheets showed that oil seeped through the sheets. On the polysilazane-coated sheets, the oil stain mark was more uniform in shape versus the scattered/panned-out stain on the pristine sheet.

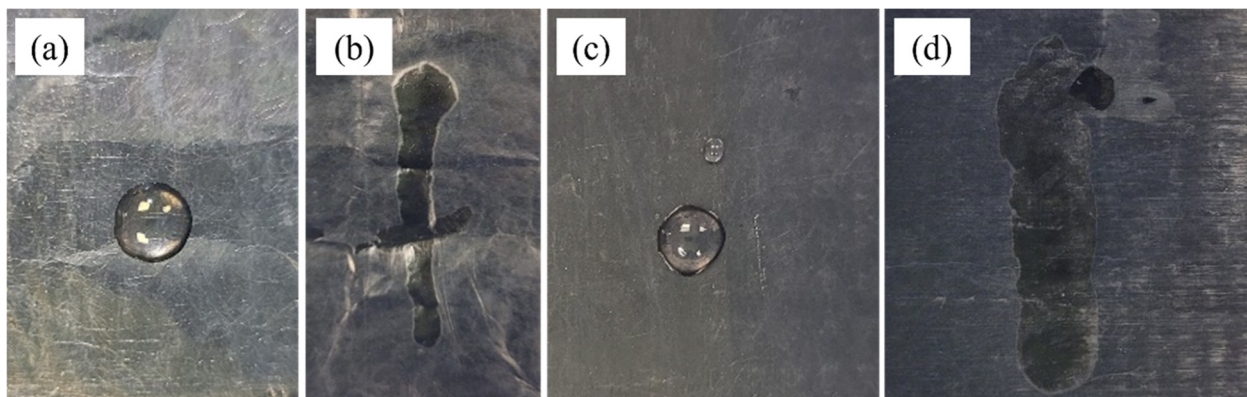


Figure 12. Hydrophobicity testing. (a) Pristine CNT sheet with water droplet. (b) Pristine CNT sheet with oil droplet. (c) Coated CNT sheet with water droplet. (d) Coated CNT sheet with oil droplet.

Water droplets placed on both the pristine and polysilazane-coated samples remained in the same position where they were placed. When the oil droplet was placed on both samples, the droplet was absorbed into the sample and started to spread throughout the sample. The polysilazane-coated CNT sample seemed to reduce the oil spreading, as the length of the oil spread was smaller than that of the pristine sample. The CNT fabrics can be characterized as oleophilic (having an affinity for oils and not for water).

2.9. Other Properties

The properties of CNT sheets depend on the synthesis method and post-processing methods such as acid treatment. Thus, the properties reported in other sources may differ from the properties reported here. Also, certain properties were not evaluated in this paper. For completeness, these other properties are reported from [2] for pristine sheets only and are taken as approximate. The thermal conductivity of pristine CNT sheets is 30–100 W/(mK) in-plane depending on density and process conditions and 0.2–4 normal to the plane (through the thickness of the sheet). In the normal direction, thermal conductivity can be as low as 0.03–0.05 if the material is loosely packed with air inside. This extreme anisotropy in thermal conductivity ranges from 150:1 to 25:1 [2]. The Seebeck coefficient ($\mu\text{V}/\text{K}$) is about -60 for n type and 70 for p type material [2].

Polysilazane-coated CNT sheets, as shown by the testing, have similar properties relative to pristine CNT sheets. Advantages of the polysilazane coating are in increasing the sheet's flame resistance and stiffness and mostly eliminating the shedding of CNT bundles. thin nonwoven polysilazane-coated CNT sheets have a unique combination of properties, and the sheets have not been fully taken advantage of in applications. Thus, ideas for possible applications are given next.

3. Applications

Different possible concept applications of CNT sheets are briefly described below. Investigating the five applications is beyond the scope of this paper.

3.1. Battery Secondary Enclosure

Fires caused by rechargeable batteries, including lithium-ion batteries, have been increasing steadily in the US. The number of fires is difficult to estimate. However, since 2019 at the earliest, fire departments in New York and San Francisco have responded to at least 669 incidents combined [14]. These fires caused 12 deaths and more than 260 injuries.

The fires occur in electric cars, e-scooters, e-bikes and other devices that use lithium-ion batteries. Once a vehicle catches fire, their lithium batteries continue to burn at extremely high temperatures by thermal runaway, which does not need oxygen from ambient air to continue burning [14–16]. Many fire departments are recommending letting the vehicle burn and extinguish itself, rather than trying to put it out [15]. As such, there needs to be a way to better encapsulate the battery such that if it were to catch fire, it would not spread throughout the vehicle.

CNT sheets demonstrated good anti-flammability characteristics when exposed to the vertical flame test. The polysilazane-coated CNT sheet did not ignite and did not exhibit material loss during a short-time flame test. This trait may be useful for electric vehicle manufacturers to enclose a vehicle's existing battery compartment to help prevent lithium fires from spreading. Another favorable characteristic of CNT sheets is their low mass. Mass reduction of electric vehicles directly translates to increased vehicle range. Electric vehicle battery fires often exceed 2500 °F [14,15]. The decomposition temperature of CNTs is about 1240 °F. However, Durazane[®] 1000 and 2000 polysilazane products [4] provide coating binders to withstand temperatures up to 1832 °F. Thus, CNT sheets could serve as a secondary enclosure in an electric vehicle's battery compartment that is lightweight and provides additional partial protection against battery fires [17].

CNT sheets may surround the batteries. An electric vehicle battery pack is made up of thousands of lithium-ion cells [16]. The cells are assembled into a battery pack that is encased in a strong material, like titanium (melting point: 3034 °F, density: 4.51 g/cc). The battery pack is normally bolted to the vehicle's undercarriage to make the battery difficult to access and to protect it during collisions. However, a severe collision can cause the battery on the bottom of the car to rupture. Polysilazane-coated CNT sheets are about 14% of the density of titanium. CNT sheets have high thermal conductivity which can help cool battery fires. Also, when CNT sheets decompose, they turn into carbon gases which are not dangerous in an open-air environment. Thus, polysilazane-coated CNT can be used as a Supplementary Materials to add shielding for electric vehicle components to protect them from burning, although polysilazane-coated CNT fabric itself cannot stop a battery fire. The enhanced safety achieved by protecting both the vehicle and its occupants and shielding combustible components in the rare event of a battery fire underscores the importance of further development and integration of CNT sheets within the electric vehicle industry. From engine bays and fuel pumps to electric batteries for new electric vehicles, coated CNT fabrics could help prevent or delay fires, explosions, or damage from high temperatures. Figure 13 shows an example of using CNT fabric to protect sodium metal from burning in water.

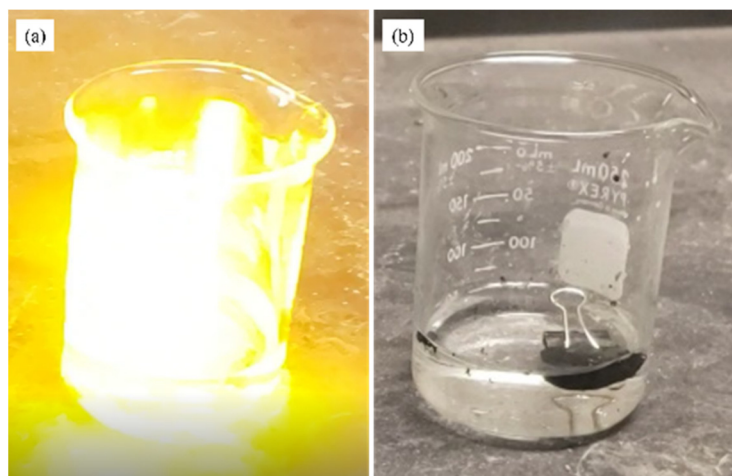


Figure 13. Alkali metal battery material with pristine CNT sheet. (a) Sodium CNT piece dropped into water in beaker. Sodium burns on the one-sided CNT fabric in water. The CNT was torn by burning but was intact. The flash burning was completed in about one second. (b) Sodium covered with two-sided CNT fabric is impermeable to water and does not react with water.

3.2. Textile Conductor for Soft Actuators

The field of soft actuation for robotics and other applications has seen significant advancement in recent years, driven by the quest to create more flexible, adaptable, and biomimetic robotic systems. CNTs could be used in the construction and actuation of robots by combining CNT sheets with a shape memory alloy (SMA) material like nitinol foil or wire to create a lightweight actuator. A CNT–SMA foil sheet actuator material could be laser cut into a desired shape and used to power a robotic end effector. This fusion of materials offers the potential to create versatile and programmable structures that can be shaped, reshaped, and actuated. Testing is required to explore the suitability of nonwoven CNT textiles for soft robotic actuation. CNT textiles' inherent suitability to work as heating/cooling elements and how they can be best fused with SMA materials to create a layered “sandwich” structure or a linear CNT–SMA structure could be explored.

The integration of nonwoven CNT textiles with SMAs like nitinol presents a new approach to soft robotic actuation. One fundamental approach involves creating a two- or multi-layer sandwich material. The layers consist of nonwoven CNT textile and SMA (nitinol foil). To create a cohesive structure, the layers are bonded together. A flexible adhesive that remains stable at high temperatures and can withstand heat cycling would be most suitable. The value of this layer structure is in its flexibility in terms of shape and motion. It can be produced in large sheets and then, by cutting and shaping the same material into any desired configuration, the SMA layer (nitinol) can return to those specific shapes upon activation and without damaging the CNT layer, within the strain range of the CNT fabric. The activation is achieved through heating action. When heated to the transition temperature or austenite finish temperature, nitinol undergoes a phase change, allowing it to revert to its original “trained” shape. This phase change can be roughly controlled to achieve desired robotic movements. Applications of this multi-layer material in soft robotics might include shaping the material into robotic arm end effectors and providing the ability to grasp and manipulate objects. The material could also be tailored into the body and limbs of small walking robots. SMA actuation allows for controlled and repeatable motion. The downside of using SMA materials is the high temperature and large power required to actuate the material. CNT fabric is uniquely compatible to use with SMA because CNT fabric can withstand high temperatures and the plastic strain of CNT fabric is large. Strain cycling of the CNT should be investigated. Another approach is to use a series CNT–SMA structure. A linear actuator design that tensions a CNT sheet is shown in Figure 14.

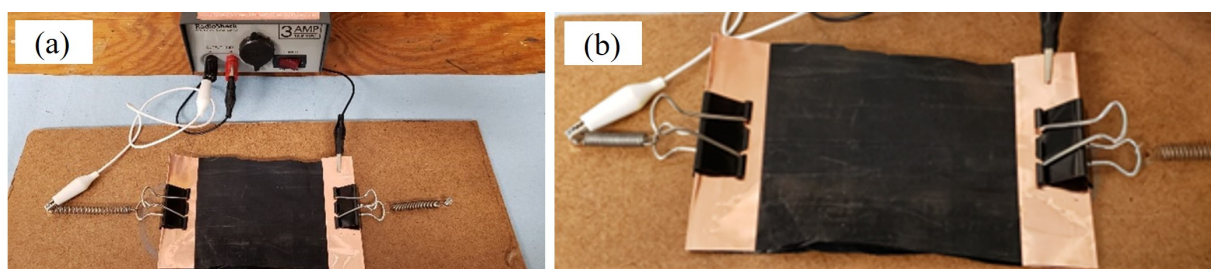


Figure 14. Illustration of a possible actuating textile. The device components are a nitinol SMA wire coil connected to a polysilazane-coated CNT sheet (with Cu strips at the ends) that is connected to a restoring spring. A 12 V power supply powers the SMA wire. The actuating textile may be useful for soft actuation, robotics, and technical or smart textiles. The CNT sheet tightens and displaces based on the stiffness of the bias spring and the length and stiffness of the SMA wire coil. (a) Before actuation (SMA spring is extended in the cold condition). (b) After actuation (SMA spring is heated and retracted). The resistance of the multi-layer CNT sheet is 2 ohms, allowing it to conduct electricity in the smart material. Supplementary Materials Video S3: Sample of SMA CNT actuator is a video of the actuation.

3.3. CNT Compositing Textiles as Shielding Materials

CNT fabric can be used in PPE such as garments to shield against environmental conditions such as high temperature/flames, toxic chemicals and smoke particles in the air, and electromagnetic waves. CNT sheets were shown to be hydrophobic, and the fabric is also impermeable to air. Since CNT fabric is also electrically conductive, it can partially shield electromagnetic waves.

An increasing number of engineered systems are producing electromagnetic waves. These items range from MRI machines, computers, cellphones, electric vehicles, an increasing number of powerlines, and microwave transmitters. While much of the research indicates that the waves emitted by these components are not harmful to humans, there is still a desire to protect against electromagnetic waves. Electromagnetic interference (EMI) overall is a problem for most electronics. Currently, metals are the most used materials for electromagnetic shielding of radio and microwaves [18–22]. Metal foils, mesh, wires, coatings, or particles can be used. Tin-plated steel is used for shielding low frequencies, copper alloy–nickel–silver is used for shielding mid-range frequencies, and copper is used for shielding both magnetic and electrical waves. Although metals provide excellent electromagnetic shielding, their high density is a limitation. Thus, CNT fabric is a strong contender in electromagnetic shielding. CNT fabric provides protection against electromagnetic fields in the radio frequency (RF) spectrum with frequencies from 3 kHz to 300 GHz.

Electromagnetic interference (EMI) is mainly an unintended effect that degrades the performance of electronic components. For example, mass transit systems may experience EMI because of electromagnetic interference from electric motors and transformers. Medical equipment including electronic surgical units, life support ventilators and infusion pumps, patient telemetry and assistance equipment, and X-ray machines for diagnostics and therapeutics is susceptible to reduced performance due to EMI. On the other hand, intentional electromagnetic interference is also becoming a threat to military and non-military equipment such as the power grid and other types of critical infrastructure. Electronic warfare EMI threats include high-altitude nuclear electromagnetic pulses (EMP) and high-power microwave (HPM) weapons.

Textiles are not natural EMI-shielding materials, but they can be modified to be electrically conductive [22]. In a study [19], conductive fillers, consisting of silver- and nickel-coated carbon fiber filler (Ni/CF), multi-wall powder CNTs, and polypyrrole nanoparticles (Ppy) were applied to fabrics individually and in combination. The results showed that the CNT- and Ppy-coated fabrics achieved EMI shielding with fewer layers than the silver- and Ni/CF-coated fabrics. Results of the combination samples showed that the CNT powder coating had the greatest effect on EMI shielding of all four coatings. The sample with the highest shielding effectiveness and lowest filler loading was a CNT+Ppy combination. Typical materials used as conductive coatings for textiles are copper, silver, nickel, and carbon. As shown in [19], CNT outperformed Ag, Ni, and C in electromagnetic shielding. EMI shielding effectiveness requirements of MIL-DTL-83528 set a minimum shielding effectiveness of 100 dB at RF frequencies between 20 and 10,000 Hz. CNT fabric has different shielding properties than CNT powder mixed in a binder. CNT fabric with different types of nanoparticles integrated into the binder is a potentially more customizable and easier to handle material for EMI shielding and needs further investigation.

Besides shielding electronics with sheets, another approach can be used. The electric field inside a charged closed metal surface of any shape is zero, if the current is zero. Free charges in the metal go to the surfaces of the metal and arrange themselves so that the electric field is zero everywhere inside the metal. A closed metal surface that screens out external sources of stray electric fields is called a Faraday cage. If there are no charges inside a closed metal surface, then the electric field inside the metal surface is zero everywhere. A Faraday cage or Faraday shield (conductive cover or mesh enclosure) is used to block electromagnetic fields [18–22] and protect sensitive electronic equipment from EMI. They are also used to protect people and equipment against actual electric currents such as lightning strikes and electrostatic discharges, since the enclosing cage conducts current

around the outside of the enclosed space and none passes through the interior. Faraday bags are a type of Faraday cage made of flexible metallic fabric and can be used to protect data storage devices from losing data due to external EMI (electromagnetic induction, electrostatic coupling, or conduction) [22]. Part of the shielding mechanism is weakening the incoming electromagnetic wave through eddy currents. This is observed when the electromagnetic wave is oscillating at a high frequency, which induces currents within the conductor. The eddy currents create a magnetic field that opposes the external magnetic field. Materials with high electrical conductivity create stronger eddy currents. CNT sheets in multiple layers with a sealant that contains metal particles is a possible flexible lightweight material for EMI shielding [23]. Figure 15 shows an EMI shield material using a polysilazane-coated CNT sheet.



Figure 15. Electromagnetic shielding of incoming and outgoing electromagnetic waves can be achieved by surrounding electronics with electrically conductive laminated polysilazane-coated CNT sheet (outer nonconductive fabrics (blue) enclose the polysilazane-coated CNT sheet (black)). As an example, a cell phone can be wrapped in three layers (75 μ thick in total, not including the thickness of the insulating outer fabrics) of polysilazane-coated CNT sheets. The phone disconnects from a call when wrapped with this sheet. The CNT sheet should always be laminated with electrically insulating sheets to add strength and prevent electrical contact of the CNT sheet.

General applications of shielding materials include carbon nanotube-based coaxial electrical cables and wiring harness, spacecraft shielding, and thermal shielding [24–26]. CNT are used for high-frequency shielding applications because the diameter of CNT bundles is smaller than the skin depth of many materials. This makes CNT better conductors and shields than metals in the GHz range. Reviews of EMI shielding are given in [27–30].

In Figure 15, experimentally showing that three layers of polysilazane-coated CNT block cell phone signals is useful design information. Polysilazane-coated CNT fabric could be laminated (stitched, bonded, welded) between two strong electrically insulating outer fabric layers and function as EMI-shielding fabric for electronic devices or enclosures. The outer fabric layers are required to protect the polysilazane-coated CNT fabric from abrasion and from contact with live electrical devices. Application prototypes must always be tested to applicable standards for safety.

3.4. Automotive Smart Fabric Components

Sealed CNT fabric can be used in several components in automotive design. Different fields of study such as textile technology, chemistry, and computer science all must work together to integrate CNT textiles into automobile applications [31–34]. Several ideas are presented below.

CNT fabric can be implemented to miniaturize the interior trims of vehicles. While focusing on sustainability, the smart textiles must integrate control and feedback functions and be equipped with electronics in the form of flexible conductors or circuit paths. A center console for a vehicle using CNT-based smart textiles could be developed by imbedding conductors and switches into CNT fabric.

A force-sensing resistor [35] can be attached to a CNT sheet to enable detection of force applied at any location along the center of the CNT sheet (Figure 16a,b). The force-sensing resistor uses interdigitated electrodes to increase the gauge factor (change in resistance/force applied) and to enable detection of forces applied at any location along the length of the sensor.

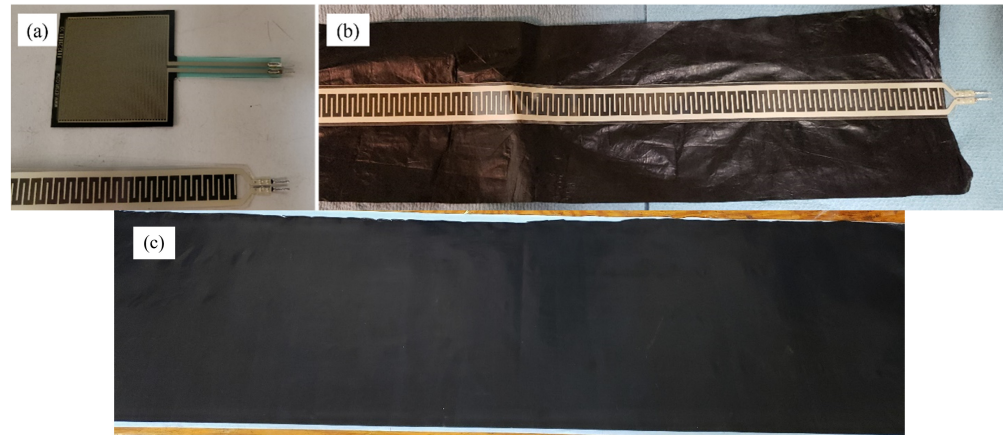


Figure 16. Force-sensing resistors (FSR) [36]. (a) Different commercial shape sensors [36] that can be integrated with CNT fabric. (b) Long force-sensing resistor integrated with CNT-silicone sheet produced at UC Nanoworld Labs [3]. The resistor can detect transverse force being applied to the CNT fabric at any location along the center of the CNT sheet. (c) EMI can be reduced using polysilazane-coated CNT sheet. The sheet must have protective outer fabric layers that are strong and electrically insulating for safety.

Fiberglass or carbon fiber body panels do not provide good grounding on automobiles. Components that normally are bolted to the frame or panels for grounding must have grounding wires integrated onto composite panels. CNT fabric near the surface of composite panels could provide grounding. CNT fabric's electrical conductivity can be increased using filler materials. Since CNT fabric is nonwoven and is not strong, it may be composited or layered with other fabrics to add strength. CNT fabric could be enclosed in Kevlar fabric to add strength and still provide static discharge and electromagnetic shielding properties to the composite fabric. Silicone is another [1] sealant that makes CNT fabric tougher and stronger.

3.5. Aircraft High-Temperature Laminated Composites

The aviation industry is constantly seeking to improve the performance, safety, and efficiency of aircraft. One of the main concerns is the choice of materials, particularly for crucial components such as aircraft composites, which must withstand rigorous conditions. One important property for aircraft is corrosion resistance. Composites are corrosion resistant. A sealant can reduce moisture absorption in composites. CNT use is already being explored for aerospace applications. The fuselage of composite aircraft is made from sheets of different composite materials that need to be fused together in huge ovens and autoclaves. Researchers have used carbon nanotubes to eliminate the need for these autoclave structures [37,38]. They applied an electric current to a thin film of CNT wrapped around the fuselage material, which heated the material and caused it to cure and fuse. This greatly reduced the amount of energy needed to manufacture it compared to using ovens. CNT is so light that it was able to be left on the material after curing without added weight concerns. If CNT was able to be used in more parts of the aircraft, it could reduce the total weight while improving other properties. An example of a high-temperature composite being formed by layers is shown in Figure 17. The fiberglass uses the RM-1066 Polyimide Prepreg System for High-Performance Aerospace Applications produced by Renegade Materials Corporation [39].

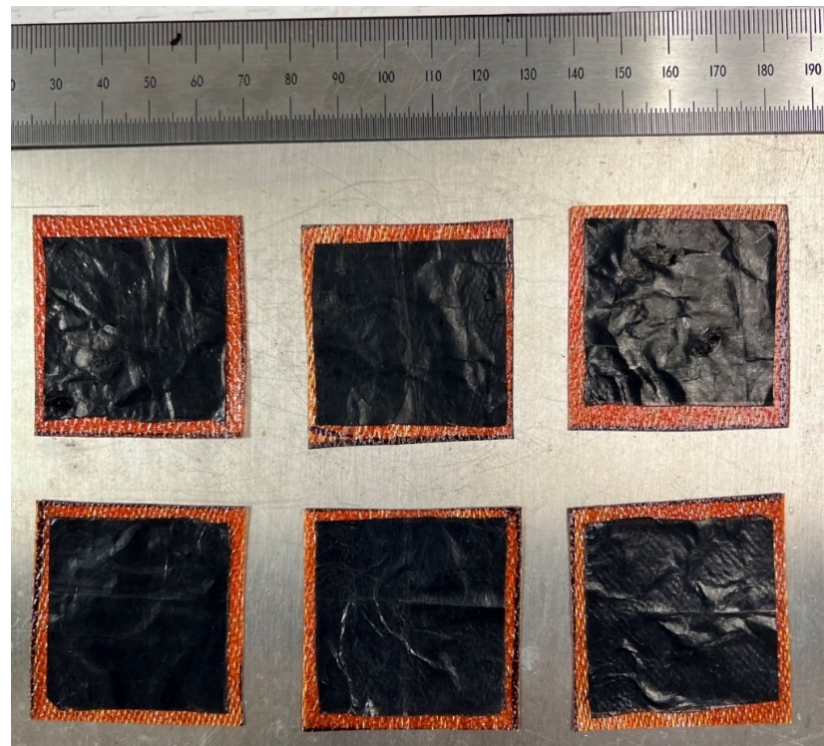


Figure 17. CNT sheet integrated within fiberglass prepreg samples for a test high-temperature composite. Six layers of high-temperature prepreg [39] with CNT sheet are used to form a high-temperature composite.

In summary, CNT fabric can be integrated into polymeric composites to increase the heat resistance, corrosion resistance, and tensile strength which could lead to greater efficiency, reduced environmental impact, and increased safety for many components of aircraft [25,26]. The CNT fabric on the samples is about 40 mm square.

4. Conclusions and Summary

This paper provides characterization results for comparing a pristine CNT sheet and a CNT sheet coated with a sealant. The results are useful in screening the materials for different possible applications. Additional testing would need to be performed to qualify the materials for specific applications. Different applications of the material are suggested. A summary of the results is given below:

1. Vertical flame test: Both the polysilazane-coated CNT and the pristine CNT demonstrated notable flame resistance. The polysilazane-coated CNT had a shorter tear length and less burn damage after exposure to a flame in comparison to the uncoated pristine CNT;
2. Average surface resistivity: Both the pristine and polysilazane-coated materials exhibited moderate electrical resistance, indicating their applicability for electrical applications such as electromagnetic shielding;
3. Tensile strength: Polysilazane-coated CNT sheets on average were stronger than pristine CNT sheer and stronger in the winding direction versus the transverse in-plane direction. Polysilazane coating reduces the shedding of CNT particles from the sheet. The polysilazane-coated CNT sheet also seems to be a more compacted CNT fabric, thus increasing the strength. CNT sheets, being nonwoven, have low strength and very high strain to failure;
4. Raman spectroscopy: The G/D ratio of the peaks for the pristine CNT sample is 7.5 and that for the polysilazane-coated CNT sheet is 4.5. The pristine sample's higher G/D ratio indicates increased crystallinity and purity (which is related to quality) of

- the CNT sheets, as polysilazane-coated CNT sheets are composed of materials other than carbon;
5. **Handleability:** The polysilazane-coated CNT sheet exhibited a comparatively higher rigidity when compared to the pristine CNT sheet and notably lacked the creases or wrinkles that were apparent in the pristine material. The polysilazane-coated CNT sheet emitted significantly less audible noise in comparison to the pristine CNT sheet when flexing the fabric. An important outcome of the study was that coated CNT almost eliminated shedding of CNT strands from the fabric;
 6. **Density:** The density for the pristine CNT was found to be 0.48 g/cc and that for the polysilazane-coated sheet was 0.65 g/cc. Thickness of the sheet was difficult to measure due to compressibility of the material, which causes error in the density calculation;
 7. **Hydrophobicity:** Both sheets are hydrophobic. The polysilazane-coated CNT fabric is more hydrophobic than the pristine CNT fabric. However, oil droplets slowly seeped through both sheets.

Further testing needed depending on the end use can be: (i) wash testing to determine if the fabric sheds particles; (ii) thermal conductivity, in-plane and along the thickness; (iii) electromagnetic shielding; (iv) chemical resistance; and (v) the Seebeck coefficient. Also, surface coating was evaluated in this paper. A coating through the entire thickness, a thicker coating, and different types of coatings may improve the properties of CNT fabric. Possible applications considered for the CNT sheets include enclosing lithium-ion batteries to reduce the spread of fires in electric vehicles, electromagnetic shielding, universal CNT-shape memory textiles for soft actuation, interiors and composite body panels of automobiles to provide electrical conduction/grounding, and protecting composite aircraft components that must withstand high temperatures. In general, CNT fabric could be a beneficial material to use in various applications including first responders (firefighters, police officers, EMT staff, etc.), welding technicians, ground military personnel, manufacturing plant workers, electrical utility workers, chefs, and other hospitality industry workers. CNT fabric composite materials can be used in shielding electronic components and in high-temperature structural applications on aircraft.

Supplementary Materials: The following supporting information can be downloaded at: <https://www.mdpi.com/article/10.3390/c10010017/s1>, Video S1: CNT Na sheet in water; Video S2: CNT Na sheet closed in water; Video S3: Example SMA–CNT actuator.

Author Contributions: Conceptualization, M.J.S. and P.G.; methodology, P.G.; validation, P.G.; investigation, P.G., I.G., M.S., A.K., A.R., B.S., A.F., J.W., K.R., E.K. and C.L.; resources, M.J.S.; data curation, P.G.; writing—original draft preparation, P.G., I.G., M.S., A.K., A.R., B.S., A.F., J.W., K.R., E.K., M.J.S. and P.G.; writing—review and editing, M.J.S.; supervision, M.J.S. All authors have read and agreed to the published version of the manuscript.

Funding: The University of Cincinnati Nanoworld Laboratories provided the use of instrumentation needed for the project. Materials for this study were provided by the National Institute for Occupational Safety and Health through the Pilot Research Project Training Program of the University of Cincinnati, Education and Research Center Grant #T42OH008432 and the Ohio Workplace Safety Innovation Center Grant WSIC24-230331-033.

Data Availability Statement: Data obtained in the research are presented in the graphs.

Acknowledgments: The authors are grateful to Melodie Fickenscher of the Advanced Materials Characterization Center, University of Cincinnati, for the support received in materials characterization. The authors are also grateful to the nanotechnologists Jack Rust and David Gailus of Huntsman Advanced Materials Company. They suggested the use of polysilazane sealant to reduce shedding of strands in the CNT sheet.

Conflicts of Interest: The authors declare no conflict of interests.

References

1. Giri, P.; Kondapalli, V.K.R.; Joseph, K.M.; Shanov, V.; Schulz, M. Manufacturing Scalable Carbon Nanotube–Silicone/Kevlar Fabrics. *Nanomaterials* **2023**, *13*, 2728. [CrossRef] [PubMed]
2. Available online: <https://www.huntsman.com/products/detail/344/miralon> (accessed on 25 November 2023).
3. Available online: <https://ceas.uc.edu/research/centers-labs/nanoworld.html> (accessed on 25 November 2023).
4. Polysilazane Suppliers: Hathaway Advanced Materials and Durazane® | Merck KGaA, Darmstadt, Germany (emdgroup.com). Available online: <https://www.hathawayresearch.com/> (accessed on 26 November 2023).
5. Available online: <https://docplayer.net/32233542-Tb1-kion-polysilazane-polyureasilazane-and-kion-polysilazane-polysilazane-20-heat-curable-resins-description-uses.html> (accessed on 26 November 2023).
6. D'Elia, R.; Dusserre, G.; Del-Confetto, S.; Eberling-Fux, N.; Descamps, C.; Cutard, T. Cure kinetics of a polysilazane system: Experimental characterization and numerical modelling. *Eur. Polym. J.* **2016**, *76*, 40–52. [CrossRef]
7. Arevalo-Fester, J. Re: Are Carbon Nano Tubes Flammable? 2014. Available online: https://www.researchgate.net/post/Are_carbon_nano_tubes_flammable/532c4a41d11b8bfe148b460a/citation/download (accessed on 26 November 2023).
8. Available online: <https://albarrie.com/products/nonwoven-meta-aramid-nomex-technical-fabric/#details> (accessed on 26 November 2023).
9. Wang, C.; Chen, F.; Kuan, S.; Chen, R.; Li, M.; Zhou, X.; Sun, Y.; Chen, D.; Wang, C. Contributed Review: Instruments for measuring Seebeck coefficient of thin film thermoelectric materials: A mini-review. *Rev. Sci. Instrum.* **2018**, *89*, 101501. [CrossRef] [PubMed]
10. Nagaraj, N. A short account of thermoelectric film characterization techniques. *Mater. Today Phys.* **2023**, *36*, 101173. [CrossRef]
11. Tang, X.; Tian, M.; Qu, L.; Zhu, S. Functionalization of cotton fabric with graphene oxide nanosheet and polyaniline for conductive and UV blocking properties. *Synth. Met.* **2015**, *202*, 82–88. [CrossRef]
12. Characterizing Carbon Materials with Raman Spectroscopy. Available online: <https://assets.thermofisher.com/TFS-Assets/CAD/Application-Notes/D19504.pdf> (accessed on 26 November 2023).
13. Sian, F.; Christopher, A.; Howard, R.; Heenan, K.; Neal, T.; Skipper, T.; Milo, S.; Shaffer, P. Scalable Method for the Reductive Dissolution, Purification, and Separation of Single-Walled Carbon Nanotubes. *ACS Nano* **2012**, *6*, 54–62.
14. Lithium-Ion Battery Fires from Electric Cars, Bikes and Scooters Are on the Rise. Are Firefighters Ready?—CBS News. Available online: <https://www.cbsnews.com/news/lithium-ion-battery-fires-electric-cars-bikes-scooters-firefighters/> (accessed on 26 November 2023).
15. Available online: <https://www.pcmag.com/news/profit-vs-the-planet-heres-why-us-automakers-are-all-in-on-electric-vehicles#:~:text=Under%20CEO%20Mary%20Barra%E2%80%99s%20%E2%80%9Czero,are%20first%20up,%20by%202030> (accessed on 26 November 2023).
16. Available online: <https://www.vox.com/the-highlight/2023/1/17/23470878/tesla-fires-eva-florida-hurricane-batteries-lithium-ion> (accessed on 26 November 2023).
17. Ng, V.; Hou, G.; Kim, J.; Beaucage, G.; Schulz, M.J. Carbon nanofabric: A multifunctional fire-resistant material. *Carbon Trends* **2022**, *7*, 100165. [CrossRef]
18. Chambers, S. Everything You Need to Know About EMI Shielding. Strouse. 17 August 2023. Available online: <https://www.strouse.com/blog/what-is-emi-shielding> (accessed on 26 November 2023).
19. Bonaldi, R.R.; Siores, E.; Shah, T. Characterization of electromagnetic shielding fabrics obtained from carbon nanotube composite coatings. *Synth. Met.* **2014**, *187*, 1–8. [CrossRef]
20. Cirino, E.; Lamoreux, K. EMF Exposure. Healthline, Healthline Media. 8 May 2023. Available online: www.healthline.com/health/emf (accessed on 26 November 2023).
21. The Modus Advanced Blog | EMI Shielding (3). Available online: <https://www.modusadvanced.com/resources/blog/topic/emi-shielding> (accessed on 26 November 2023).
22. Blachowicz, T.; Wójcik, D.; Surma, M.; Magnuski, M.; Ehrmann, G.; Ehrmann, A. Textile Fabrics as Electromagnetic Shielding Materials—A Review of Preparation and Performance. *Fibers* **2023**, *11*, 29. [CrossRef]
23. Available online: <https://www.uc.edu/news/articles/2023/09/ohio-grant-gives-uc-researchers-over-25-million-in-total-to-research-firefighter-protective-gear.html> (accessed on 26 November 2023).
24. Available online: <https://patents.google.com/patent/US9396829B2/en> (accessed on 26 November 2023).
25. Rawal, S.; Brantley, J.; Karabudak, N. Development of carbon nanotube-based composite for spacecraft components. In Proceedings of the RAST 2013 6th International Conference on Recent Advances in Space Technologies, Istanbul, Turkey, 12–14 June 2013; pp. 13–19. [CrossRef]
26. Zhe, L.; Ayou, H.; Songlin, Z.; Yourri-Samuel, D.; Liang, R. Lightweight carbon nanotube surface thermal shielding for carbon fiber/bismaleimide composites. *Carbon* **2019**, *153*, 320–329.
27. Chung, D.D.L. Materials for electromagnetic interference shielding. *Mater. Chem. Phys.* **2020**, *255*, 123587. [CrossRef]
28. Subhash, B.; Kondawar, P.; Modak, R. Chapter 2—Theory of EMI Shielding; Kuruvilla, J., Runcy, W., Gejo, G., Eds.; Materials for Potential EMI Shielding Applications; Elsevier: Amsterdam, The Netherlands, 2020; pp. 9–25. ISBN 9780128175903. [CrossRef]
29. Available online: <https://www.iqsdirectory.com/articles/emi-shielding.html> (accessed on 26 November 2023).

30. Seyyed, A.H.; Ahmadreza, G.; Ehsan, H.; Sonia, B.; Parisa, N.; Navid, O.; Seyyed, M.M.; Majed, A.; Mehrorang, G.; Seeram, R.; et al. Recent progress on hybrid fibrous electromagnetic shields: Key protectors of living species against electromagnetic radiation. *Matter* **2022**, *5*, 3807–3868. [CrossRef]
31. Elnashar, E. Functional Textiles for Airbags in Automotive Industrial. Academia.Edu. 19 March 2016. Available online: www.academia.edu/23437947/Functional_textiles_for_airbags_In_Automotive_Industrial?auto=download (accessed on 27 November 2023).
32. Powell, N.B. Design of automotive interior textiles. In *Textile Advances in the Automotive Industry*; Elsevier Science: Amsterdam, The Netherlands, 2008; p. 113.
33. Redaktion. Reutlingen University: User-Friendly Textile-Based Interactive Car Interior Using Bio-Based Materials. 12 May 2021. Available online: www.textiletechnology.net/technology/trendreports/reutlingen-university-user-friendly-textile-based-interactive-car-interior-using-bio-based-materials-30251 (accessed on 27 November 2023).
34. Arora, S.; Rekha, M.Y.; Gupta, A.; Srivastava, C. High corrosion resistance offered by carbon nanotubes directly grown over mild steel substrate. *Microsc. Microanal.* **2019**, *25*, 750–751. [CrossRef]
35. Electronic Sensors. Force Sensing Resistor (FSR). Available online: <https://www.tekscan.com/blog/flexiforce/how-does-force-sensing-resistor-fsr-work> (accessed on 26 November 2023).
36. Available online: <https://www.interlinkelectronics.com/force-sensing-resistor> (accessed on 27 November 2023).
37. Available online: <https://news.mit.edu/2020/carbon-nanotubes-making-airplane-aerospace-parts-1013> (accessed on 25 November 2023).
38. Available online: <https://physicsworld.com/a/carbon-nanotubes-bring-aircraft-manufacturing-out-of-the-oven/> (accessed on 25 November 2023).
39. Adhesive & Prepreg Supplier for the Aerospace Market | Renegade Materials. Available online: <http://www.renegadematerials.com/> (accessed on 25 November 2023).

Disclaimer/Publisher’s Note: The statements, opinions and data contained in all publications are solely those of the individual author(s) and contributor(s) and not of MDPI and/or the editor(s). MDPI and/or the editor(s) disclaim responsibility for any injury to people or property resulting from any ideas, methods, instructions or products referred to in the content.